SOPHISTICATION OF DOPING PROFILE MANIPULATION
- EMITTER PERFORMANCE IMPROVEMENT WITHOUT ADDITIONAL PROCESS STEP -

Yuji Komatsu[1], Arno F. Stassen[1], Peter Venema[2], Ard H.G. Vlooswijk[2], Christine Meyer[3], and Michiel Koorn[1]
[1]ECN Solar Energy, P.O. Box 1, NL-1755 ZG Petten, the Netherlands, Tel: +31 224 564303; Fax: +31 224 568214;
[2]Tempress Systems BV, Radeweg 31, NL-8171 MD Vaassen, the Netherlands;
[3]Solland Solar Cells BV, Avantis, Bohr 10, NL-6422 RL Heerlen, the Netherlands,
Email: komatsu@ecn.nl

ABSTRACT: We have improved the emitter formation process by manipulating the phosphorus doping profile without increasing the total process time or adding any extra steps, but by just implementing a simple steam generator into the $POCl_3$ diffusion furnace. An average efficiency gain of 0.3% absolute was achieved with multicrystalline silicon solar cells. In this study, we statistically clarify which direction the doping profile should be manipulated. Merely characterizing the emitter by "high sheet resistance" or "shallow emitter" is revealed to be no longer indicative for high efficiency. We also demonstrate the sophistication of the doping profile manipulation with numerical analysis.
Keywords: doping profile, $POCl_3$, steam

1 INTRODUCTION

The emitter formation process in the manufacture of crystalline silicon solar cells is full of dilemmas.

One can increase the cell efficiency through the modification of the emitter process by taking more time, adding several steps, and requiring a narrower process window —typically, precise alignment in the metallization process— to the subsequent processes. But the extension of the emitter process strongly influences the total manufacturing cost since the emitter process is the most time-consuming process for a wafer to become a solar cell. On the other hand, if one wants a significant efficiency increase, the total time for the emitter process also has to be increased significantly. Implementing such a process modification into a commercial production line is always accompanied by a complicated trade-off which also includes an additional consideration on sacrificing the production yield.

From the theoretical point of view, it is well known that an emitter with higher sheet resistance can give the cell a larger current and a higher voltage because the lower doping concentration and/or the shallower junction prevent unfavorable carrier recombination. However, the higher sheet resistance hinders the lateral movement of the majority carrier in the emitter and the lower doping concentration causes higher contact resistance between the emitter and the metal, both of which increase the series resistance and decrease the fill factor (FF). One of the solutions of this problem is a "selective-emitter" concept [1], which requires a complicated trade-off to implement as mentioned above. As a matter of fact, industrial manufacturers are strongly wishing for a "Holy Grail" that can improve just the emitter doping profile without increasing the total process time, adding any extra process steps, narrowing the subsequent process window, or sacrificing the production yield. A process improvement with the least risk is the most desired.

In the last EU-PVSEC, we demonstrated an efficiency gain of 0.2% absolute without adding any process steps or extending the total process time [2]. We modified the phosphorus diffusion process using a quartz tube furnace by employing a multi-plateau temperature profile instead of the conventional single-plateau temperature profile, which enabled manipulation of the doping profile resulting in the decrease of the doping concentration near the emitter surface. The efficiency gain was due to the increase of the short circuit current (J_{sc}) and the open circuit voltage (V_{oc}), and the FF was kept as large as the conventional one's.

In this study, the correlation between the solar cell performance and the doping profile is more precisely investigated. At the same time, the manipulation of the doping profile has been sophisticated. We indicate which part of the doping profile influences the solar cell performance, and to which direction and how it should be manipulated.

2 EXPERIMENTS

To investigate the correlation between the solar cell performance and the doping profile, the phosphorus diffusion processes of different experiment groups should be compared accurately. At the same time, the manufactured solar cell should be equivalent to a commercial product; otherwise the obtained correlation will not give a solution to the "manufacturers' dilemmas". A polished surface is necessary in order to characterize a doping profile, even with state-of-art techniques, which means that the doping profile of an actual solar cell cannot be characterized since the surface is textured. Therefore, we put a surface-polished wafer into the diffusion furnace together with the cells of each experiment group. The doping profile characterized with the surface-polished wafer should have a one-to-one correlation with the emitter profiles of the actual cells of each group.

The diffusion tool is an industry-scale $POCl_3$ tube furnace Tempress TS81003, equipped with 400 slots for loading 156×156 mm² wafers in its temperature flat zone. We implemented a steam generator RASIRC® Steamer 125 [3] into the $POCl_3$ furnace in order to widen the process possibility, or in other words, to sophisticate the doping profile manipulation. To our best knowledge, implementation of a steam generator into the $POCl_3$ diffusion process for manufacturing solar cells has not been reported before this study.

The doping profile of the surface-polished wafers were characterized with secondary ion mass spectroscopy (SIMS) carried out by Philips MiPlaza [4]. There are two other well-known methods to characterize doping profiles: ECV (electrochemical capacitance voltage) and SRP (spreading resistance profile); but SIMS is the most

appropriate for phosphorus diffusion because the impact of electrically inactive dopant cannot be neglected. The repeated measurements of the same diffusion process carried out in different months showed a good agreement, which suggests the reproducibilities of both the diffusion furnace and the SIMS measurement are reliable.

21 groups of different phosphorus diffusion processes were tested including the reference group. The temperature profile of the reference group has a single temperature plateau as shown in Fig.1 (a) which is conventionally used in industrial production lines. A typical temperature profile out of 20 test groups has multiple temperature plateaus as shown in Fig.1 (b). To analyze the processes and the results numerically, four control parameters were selected to vary, including the use of steam, and the other process parameters were fixed as strictly as possible. The total process time for each test groups is almost same as the reference and the diffusion uniformity through the whole furnace is sufficiently good.

Polished CZ Si (110) wafers out of one single lot were used to characterize the doping profiles, and 156×156 mm² multicrystalline silicon wafers were used for manufacturing solar cells. Except for the phosphorus diffusion process, the other process steps —like texturing, SiN_x deposition, metallization, etc.— were the same for all samples and processed in one time to the utmost. Neighboring wafers were equally distributed to each group. Since the wafers were arranged from three different ingots, the values of J_{sc} and V_{oc} were leveled using the average values of the reference group of each ingot. We empirically know such leveling of J_{sc} and V_{oc}

is effective enough when the emitter quality is tested independently.

3   RESULTS

The four graphs of Fig.2 show the doping profiles characterized by SIMS. Each graph shows the profiles of the reference and 5 selected groups. The values showed
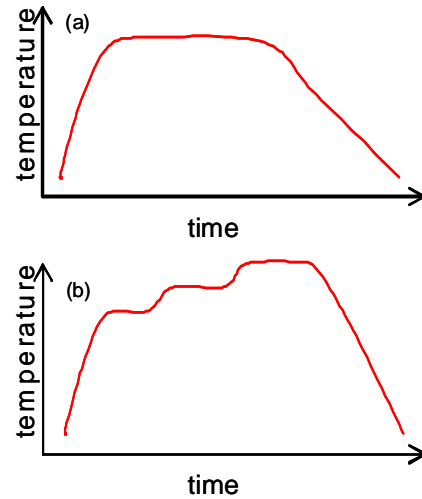

Figure 1: (a) Single-plateau temperature profile conventionally used in industrial production lines. (b) Typical multi-plateau temperature profile employed in this work.
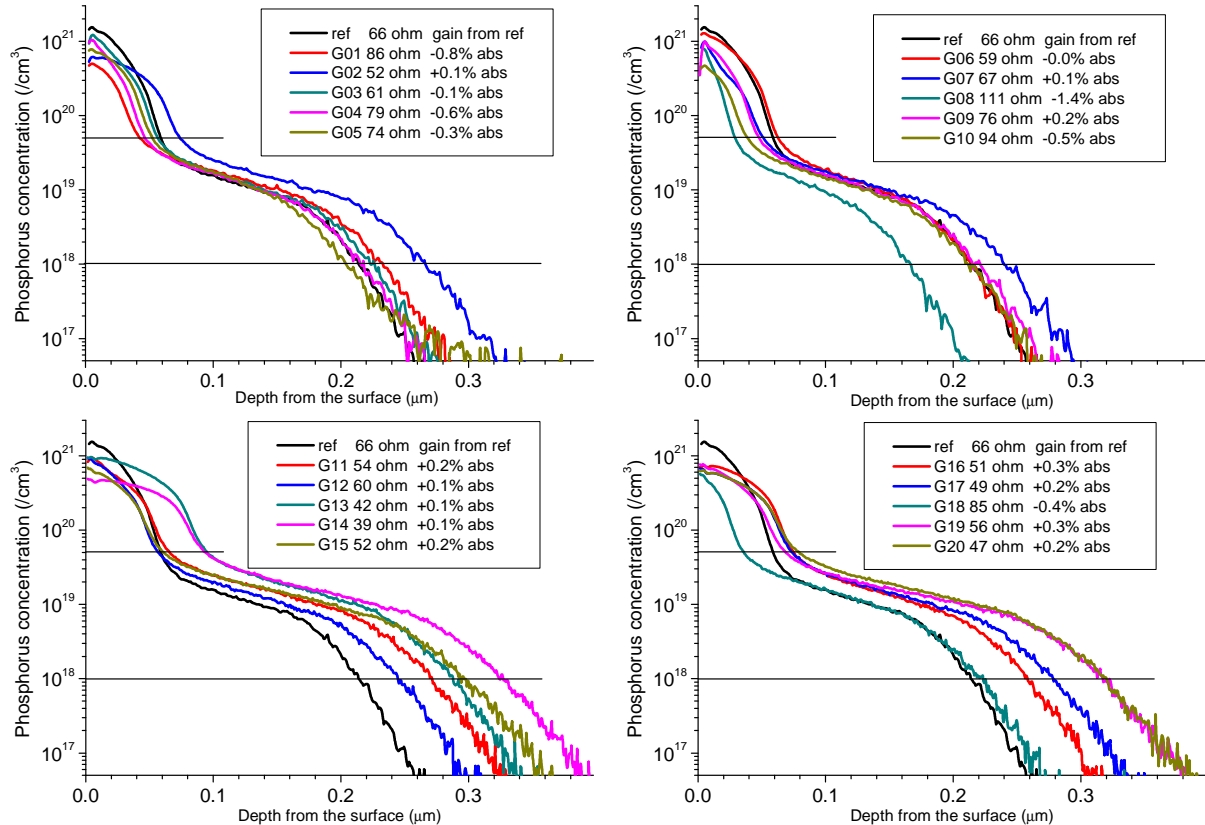

Figure 2: Doping profiles characterized by SIMS. Each graph shows the profiles of the reference and 5 selected groups. The values shown in the legend boxes are sheet resistance of a cell out of the same group measured before SiN_x deposition, and the average of the absolute efficiency gain of the specific group compared to the reference group.

Table I: Numerically expressed doping profiles with sheet resistance, number of the completed cells, and the average efficiency gain from the reference of each group.

	$R_\square$ $(\Omega/\square)$	doping profile			# of cells	gain from ref. $(\%_{abs})$
		x: peak density $(/cm^3)$	y: depth @5×10^{19} (μm)	z: depth @1×10^{18} (μm)		
G01	86	5.1×10^{20}	0.042	0.231	5	-0.8
G02	52	6.3×10^{20}	0.074	0.264	4	+0.1
G03	61	1.3×10^{21}	0.057	0.227	5	-0.1
G04	79	1.1×10^{21}	0.046	0.219	6	-0.6
G05	74	7.9×10^{20}	0.053	0.204	6	-0.3
G06	59	1.3×10^{21}	0.064	0.216	6	-0.0
G07	67	1.0×10^{21}	0.052	0.241	6	+0.1
G08	111	8.1×10^{20}	0.029	0.167	6	-1.4
G09	76	1.0×10^{21}	0.049	0.222	6	+0.2
G10	94	4.8×10^{20}	0.040	0.216	6	-0.5
G11	54	9.5×10^{20}	0.067	0.272	10	+0.2
G12	60	1.0×10^{21}	0.057	0.245	12	+0.1
G13	42	1.0×10^{21}	0.095	0.288	11	+0.1
G14	39	5.1×10^{20}	0.095	0.325	12	+0.1
G15	52	7.4×10^{20}	0.061	0.300	10	+0.2
G16	51	7.7×10^{20}	0.075	0.262	12	+0.3
G17	49	7.4×10^{20}	0.074	0.279	12	+0.2
G18	85	6.3×10^{20}	0.036	0.224	11	-0.4
G19	56	8.2×10^{20}	0.069	0.316	11	+0.3
G20	47	6.5×10^{20}	0.080	0.320	11	+0.2
ref.	66	1.6×10^{21}	0.060	0.215	18	—

Figure 3: J_{sc}, V_{oc}, FF, and Efficiency plots of each group with means and 95% Tukey HSD (honestly significant difference) intervals, arranged with Table I.

in the legend box are sheet resistance of a cell (average of 7×7 points) out of the same group measured by Sherescan [5] before SiN_x deposition, and the average of the absolute efficiency gain of the specific group compared to the reference group. The highest gain of 0.3% was achieved with G19, which exceeded our last result of 0.2% [2].

In comparison with the reference group, differences of sheet resistance are understandable from the doping profiles because sheet resistance is a direct outcome of the doping profile. The correlation with the efficiency gain is not straightforward, however. Surprisingly, the efficiency can be increased even if the sheet resistance is lower than that of the reference group. For instance, G02, G11, G15, G16, G17, G19 and G20 have significantly higher efficiency in spite of their low sheet resistance. So far, low sheet resistance had been regarded as a negative factor for solar cell performance, but this indicator is not always true as demonstrated in this study. It shows the solar cell performance can be more strongly correlated with the doping profile itself than with the sheet resistance value.

Figure 3 shows the plots of each factor of the solar cell performance with means and 95% Tukey honestly significant difference intervals. Most of the test groups show higher V_{oc} than the reference group while J_{sc} and FF are not always larger. This result shows that the aim of implementing multi-plateau temperature profiles: *i.e.* to reduce the unfavorable carrier recombination by decreasing the total doping and to raise the V_{oc}, has almost been accomplished. On the other hand, several groups with significantly high V_{oc} like G01, G10, and G18 lag in efficiency as compared to the reference due to the smaller FF. The groups with a larger gain such as G02, G11, G15, G16, G17, G19 and G20 have a FF as large as the reference.
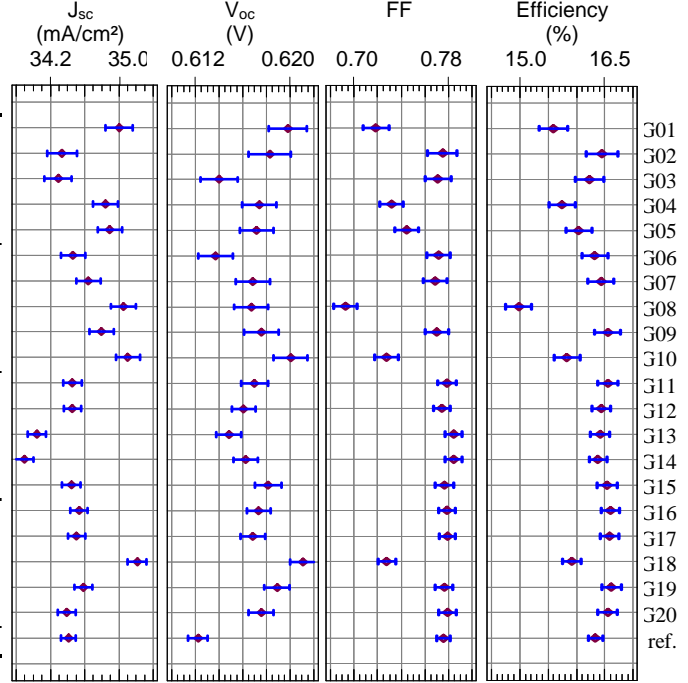
4 DISCUSSION

4.1 Definition of analysis method

To carry out the analysis more quantitatively, the doping profile curves should be numerically expressed. With a glance at Fig.2, one can easily recognize that all the curves are composed of two Gaussian-like curves. The amplitude of the first Gaussian-like peak is variable with the peak occurring at the surface. The amplitude of the second Gaussian-like peak appears to be common for all the curves. This is because the diffusivity of phosphorus ($D_{[P]}$) at the phosphorus concentration ($[P]$) of 1×10^{19} /cm³ is 5 ~ 7 times larger than the $D_{[P]}$ at $[P] = 1\times10^{20}$ /cm³ [6]. Therefore two Gaussian-like curves appear: one starts at the surface and the other starts at $[P] \sim 3\times10^{19}$ /cm³. The peak concentration of the first curve depends on each diffusion condition. This causes the formation of two different layers with different $[P]$, which are called n^{++} and n^{+} layers as shown in Fig. 4.

Normally, one can describe a Gaussian curve with two variables which are the peak concentration and the depth factor. In the case of Fig. 2, each doping profile
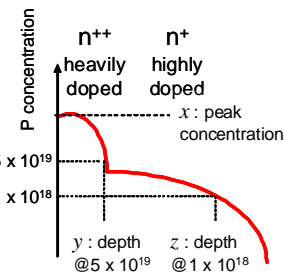

Figure 4: Simplified model of phosphorus doping profile formed by diffusion process. Variables *x*, *y*, and *z* are also indicated.

Table II: β_n/ε_n (ratio of [coefficient] / [standard error]), P-value (indicating statistical significance when close to zero), and adjusted R^2 (representing the percentage of the variability) of the main solar cell characteristics derived from statistical fitting by linear regression analysis for the model with equation (1).

	J_{sc}		V_{oc}		FF		Efficiency	
	β_n/ε_n	P-value	β_n/ε_n	P-value	β_n/ε_n	P-value	β_n/ε_n	P-value
x: n^{++} peak concentration	-6.4	0.000	-11.3	0.000	10.0	0.000	6.2	0.000
y: n^{++} depth @5×10^{19} /cm³	-11.5	0.000	-7.9	0.000	5.2	0.000	0.6	0.540
z: n^{+} depth @1×10^{18} /cm³	-1.4	0.163	4.3	0.000	6.7	0.000	6.6	0.000
adjusted R^2	75.1%		65.8%		71.7%		47.8%	

can be distinctly described with three variables because the peak of the second Gaussian-like curve is common with ~3×10^{19} /cm³. In this study, we used three variables of

x : peak concentration,
y : depth at [P] = 5×10^{19} /cm³,
z : depth at [P] = 1×10^{18} /cm³,

as a quick numerical expression of a doping profile as indicated in Fig. 4. Variables x and y describe the peak and the depth of the n^{++} layer, respectively, and z describes the depth of the n^{+} layer.

Although this description does not accurately represent the two Gaussian-like curves, it should be meaningful as a first approximation. Table I summarizes the numerical expressions of the doping profiles with the variables $x \sim z$ described above, together with sheet resistance, number of the completed cells, and the average efficiency gain from the reference of each group.

We carried out linear regression analysis using STATGRAPHICS Centurion XV [7] for the main characteristics of the solar cell performance —J_{sc}, V_{oc}, FF, and efficiency— with these variables expressing each doping profile. In this analysis, each cell factor was statistically fitted with a linear model expressed with the next equation:

$$W = \beta_0 + \beta_1 x + \beta_2 y + \beta_3 z + \varepsilon , \quad (1)$$

where, W is either of J_{sc}, V_{oc}, FF, or efficiency; β_n are statistically estimated coefficients; and ε is the residual error. Each estimated coefficient accompanies a standard error ε_n and P-value. The ratio β_n/ε_n indicates relative weight of each variable in equation (1) and can be used for the comparison of each variable's contribution to W. The P-value indicates the statistical significance of each coefficient when it is close to zero. Normally, the coefficient can be regarded as statistically significant when P-value < 0.05. Each equation (1) for each W accompanies R^2 which represents the percentage of the variability in W which has been explained by the fitted regression model, ranging from 0% to 100%. In this analysis, R^2 is adjusted for the number of coefficients.

4.2 Discussion of analysis results

Table II summarizes β_n/ε_n, P-value, and adjusted R^2 of the main solar cell characteristics. The plus/minus of β_n/ε_n indicates the direction of the contribution of the variable. A positive sign means an increase in depth or height is favourable while a negative sign indicates a decrease is favourable. Most of the P-values are close to zero, which suggests the overall analysis is statistically significant enough. The R^2 values are also large enough in spite of other factors causing errors like the long manufacturing process potentially prone to induce

instability, wafer quality variation in an ingot, unexpected deviation from average at the SIMS measurement point, etc.

Hereafter, the results are discussed for each element.

J$_{sc}$, short circuit current

All three variables x, y, and z have negative coefficients, which means J_{sc} will increase with a lower n^{++} peak, a shallower n^{++} layer, and a shallower n^{+}. These are all easily understandable because the heavily doped n^{++} and n^{+} layers are regarded like nests of carrier recombination centres while many of the incident photons generate electron–hole pairs within the emitter. Therefore, some part of the photo-generated minority carriers are recombined before being transported from the emitter to the base, resulting in smaller J_{sc}.

V$_{oc}$, open circuit voltage

Like J_{sc}, V_{oc} will also increase with a lower n^{++} peak and a shallower n^{++} layer. In most part of the n^{++} layer, the phosphorus dopant concentration is higher than 1×10^{20} /cm³ where the impact of Auger recombination is hardly avoided. Even worse, the excess dopant higher than $3\sim5\times10^{20}$ /cm³ is electrically inactive and creates Shockley-Read-Hall (SRH) recombination centers in the layer. Interface SRH recombination centers are created even by lower dopant concentration than this. Such recombination sources generate thermal minority carriers and increases the dark saturation current of the solar cell device, resulting in lower V_{oc}.

The n^{+} depth functions in an opposite way: the V_{oc} will increase with a *deeper* n^{+} layer. In the n^{+} layer, almost all the phosphorus dopant is electrically activated and the impact of Auger recombination is small because of the low concentration compared to the n^{++} layer. In addition, the distance between the n^{++} and the pn-junction contributes to the decrease of the dark saturation current, which can be explained as follows: At the dark condition, fewer minority carriers thermally generated at the n^{++} layer can reach the pn-junction because the recombination probability in the n^{+} layer increases with the n^{+} layer being thicker, even though it is paradoxical. This phenomenon is demonstrated in this study by a considerable value of positive β_n/ε_n accompanied by a zero P-value.

FF, fill factor

The trends of all the variables are completely opposite when comparing FF and J_{sc}. FF is known to be increased with decreasing series resistance. A higher n^{++} peak and a deeper n^{++} layer will reduce the contact resistance between the emitter and the metal, and both deeper n^{++} and n^{+} layers increase the lateral conductivity of the majority carrier. Thus, these results with positive coefficients are well understandable.

Efficiency

As discussed so far, the trends of the doping-profile variables have brought us another "manufacturers' dilemma". The trends of all the variables have both positive and negative impact on either of J_{sc}, V_{oc}, and FF. This means that trade-offs are needed to adjust all the doping-profile variables considering the weight on all the main solar cell characteristics.

The values in the "Efficiency" columns of Table II imply a key for this trade-off. The small β_n/ε_n and the large P-value for y (n^{++} depth) suggest that change of n^{++} depth will not have a large impact on the efficiency. On the other hand, both x (n^{++} peak) and z (n^+ depth) have large and positive β_n/ε_n with zero P-values, so x and z had better be increased.

With this knowledge, the original doping profiles in Fig.2 are looked at again, especially the promising groups of G16, G17, G19 and G20, and several groups with distinctive features of G09 and G10. Relatively deep n^+ layers are seen for G16, G17, G19 and G20, which suggest the deeper n^+ contributed to raising efficiency. They have significantly higher efficiency than the reference even though they have both deeper n^+ and n^{++}. This also supports that a shallower emitter is not always a solution to improve the solar cell performance.

Both G09 and G10 have very similar curves to the reference at the n^+ layer while both have lower n^{++} peaks and shallower n^{++} than the reference. Very interestingly, G09 gains 0.2% while G10 loses 0.5% despite this small difference. The main cause of the efficiency loss of G10 can be known as a large drop of FF shown in Fig. 3. On the other hand, the n^{++} profile like G09 (or G07) still can render sufficiently high FF.

As already mentioned, the largest gain was obtained with G19 as 0.3% absolute. But what if the n^{++} looks like G09 and the n^+ looks like G19? Still, a lot of combinations are not yet tested and the efficiency improvement can be expected through such attempt.

5 DOPING PROFILE MANIPULATION

As mentioned in the previous section, 20 different diffusion processes were designed and carried out. To analyze the processes and the results numerically, four control parameters were selected to vary, including the use of steam. The other process parameters were fixed as strictly as possible, and the total process time for the test groups are similar. The diffusion uniformity through the whole furnace is sufficiently good even when steam is introduced into the process.

Linear regression analysis using STATGRAPHICS was carried out again for each variable of the doping profiles as functions of process parameters. Each doping-profile variable was statistically fitted with a linear model expressed with the next equation:

$$w = \gamma_0 + \sum_{n=1}^{4} \gamma_n X_n + \varepsilon, \qquad (2)$$

where, w is either of x, y, or z; γ_n are statistically estimated coefficients; and X_n are the process control parameters. Like in the previous analysis, each coefficient accompanies standard error ε_n and P-value, and γ_n/ε_n and P-value are used to evaluate the statistical

Table III: γ_n/ε_n, P-value, and adjusted R^2 of each doping-profile variable derived from statistical fitting as a function of process control parameters X_n by linear regression analysis for the model with equation (2).

	x: n^{++} peak concentration		y: n^{++} depth @5×10^{19} /cm³		z: n^+ depth @1×10^{18} /cm³	
	γ_n/ε_n	P-value	γ_n/ε_n	P-value	γ_n/ε_n	P-value
X_1	0.0	0.994	5.5	0.000	8.6	0.000
X_2	-2.6	0.019	-8.6	0.000	-2.1	0.051
X_3	5.4	0.000	-0.5	0.607	-2.3	0.033
X_4	0.5	0.659	5.1	0.000	4.7	0.000
R^2	60.7%		90.2%		92.6%	

significance.

Table III summarized the results of the linear regression analysis. Both R^2s of the n^{++} and n^+ depths (y and z) are larger than 90%, which suggests these depths are well controlled with the process parameters. X_1 and X_4 have strong correlation with both depths (y and z) and X_2 also looks decisive of the n^{++} depth (y) since all of their P-values are zero. By exploiting X_1 and X_2, for instance like G18 in Fig. 2, the depth ratio of n^{++}/n^+ (y/z) can be differentiated to the extent which was impossible without introducing steam.

The controllability of the n^{++} peak (x) does not look as accurate as the depths since R^2 is not so large. On the other hand, the weak correlation of the peak (x) with X_1 and X_4 allows much freedom of independent control of the depths (y and z) from the peak (x) by tuning X_1 and X_4. The same will be also true for X_3 to control the peak (x).

Overall, control of these doping-profile variables — or in other words, manipulation of the doping profile— has been sophisticated with these four process control parameters. We are now able to produce pre-designed doping profiles by this means. Also, implementing a steam generator into a POCl$_3$ tube furnace is demonstrated to improve the doping profile manipulation without increasing the total process time, adding extra process step, or narrowing process window at the subsequent process. The latest achievement is an average efficiency gain of 0.3% absolute.

As a further attempt to target even higher efficiency gain, a wider range for these control parameters should be assessed, and several conditions fixed in this study should also be varied.

6 CONCLUSION

The phosphorus doping profile in the emitter was characterized and the correlation between the profile and the solar cell performance was numerically investigated using statistical analysis.

Three variables were chosen to express the profile curve, which represent the peak concentration, the n^{++} layer depth, and the n^+ layer depth, respectively.

The calculated correlations between these three variables and J_{sc}, V_{oc}, and FF were all seen to be statistically significant. All the trends of the three variables to increase J_{sc} were negative while they are positive to increase FF. To raise V_{oc}, the trends of the peak and the n^{++} depth were negative and that of the n^+ depth was positive.

The direction to increase the efficiency, which had

been regarded unclear because it should be an outcome of a trade-off, was also shown. The trends of the peak concentration and the n^+ depth were positive while the correlation between the efficiency and the n^{++} depth was not statistically significant.

The largest average efficiency gain from the conventional diffusion process was 0.3% absolute which was achieved in one experiment group while several groups also achieved comparable gains larger than 0.2%. Surprisingly, most of these groups had over 10 Ω/square lower sheet resistance and deeper emitter depth than the reference group with the conventional diffusion process. Merely characterizing the emitter by "high sheet resistance" or "shallow emitter" is no longer indicative for high efficiency.

A steam generator was implemented into the $POCl_3$ diffusion furnace to sophisticate the doping profile manipulation. The correlations between the process control parameters and the three variables representing each doping profile were numerically investigated using statistical analysis.

The calculated correlations suggested that both the n^{++} and n^+ depths look to be well controlled by a few of the process parameters. It was also suggested that the depth ratio of n^{++}/n^+ can be differentiated to the extent which was impossible without introducing steam.

Although the controllability of the peak did not seem as accurate as the depths, a strong correlation was observed with another process parameter which does not link strongly to the depths. This suggested the peak can be controlled independently from the control of the depths to some extent.

The doping profile manipulation was sophisticated, and further improvement is still expected.

REFERENCES

[1] *For example,* F. Book, A. Dastgheib-Shirazi, B. Raabe, H. Haverkamp, G. Hahn, and P. Grabitz, "*Detailed analysis of high sheet resistance emitters for selectively doped silicon solar cells*", 24th EU-PVSEC (Hamburg, 2009) 2CV.5.3, pp. 1719-1722.

[2] Y. Komatsu, G. Galbiati, M. Lamers, P. Venema, M. Harris, A.F. Stassen, C. Meyer, M. van den Donker, and A. Weeber, "*Innovative diffusion processes for improved efficiency on industrial solar cells approached by doping profile manipulation*", 24th EU-PVSEC (Hamburg 2009) 2CO.3.1, pp. 1063-1067.

[3] http://www.rasirc.com

[4] http://www.miplaza.com

[5] http://www.sunlab.nl

[6] A. Bentzen, A. Holt, J.S. Christensen, and B.G. Svensson, "*High concentration in-diffusion of phosphorus in Si from a spray-on source*", J. Appl. Phys., 99, 064502 (2006).

[7] http://www.statgraphics.com